

Ground-state grating echoes from Rb vapor at room temperature

A. Kumarakrishnan, U. Shim, S. B. Cahn, and T. Sleator

Department of Physics, New York University, 4 Washington Place, New York, New York 10003

(Received 25 August 1997)

We have used two sets of opposite circularly polarized traveling wave pulses separated in time to establish, and subsequently rephase, a spatially modulated coherence between the magnetic sublevels of the $F=3$ ground state in Doppler broadened ^{85}Rb vapor. The rephasing results in a magnetic grating echo whose duration is an accurate measure of the velocity distribution. We demonstrate that the time scale of the experiment is determined solely by the transit time of atoms across the laser beam. The shortening of the lifetime due to a perturber (Ar) allows us to infer the Rb-Ar velocity changing collision cross section. [S1050-2947(98)02511-6]

PACS number(s): 32.80.Pj, 03.75.Dg, 42.50.Md, 52.20.Hv

There have been several recent proposals for experiments involving grating echoes [1–4] in which a sequence of pulses separated in time creates spatially periodic atomic populations or coherences that may be subsequently rephased. The use of echo techniques for detecting collisions involving small velocity changes in Doppler broadened vapor is well known [5–7].

The excitation pulses in an echo experiment may be traveling waves as in a two-pulse photon echo [8] or standing waves, which produce spatially modulated populations (gratings) involving either excited states [9] or the ground states [10]. Alternatively, the excitation may consist of two simultaneous traveling waves with orthogonal polarizations, producing a spatially periodic coherence grating associated with the excited state [11] or the ground state as in this work and Ref. [12]. In [1,3,4,9,11,13] as well as in this paper, the formation of the echo can be explained by treating the motion of the atomic center of mass and the electric fields classically. The points of echo formation represent the cancellation of the accumulated Doppler phase of various spatial harmonics. The entire distribution of velocities that are initially excited may subsequently be rephased at the echo points.

The time scale of experiments that involve an excited state is typically limited by the excited state radiative decay time. For a coherent superposition of atomic ground states, however, the time scale should be limited only by an effective ground-state lifetime, which is limited by the transit time of atoms through the region of interaction, and by collisions. The possibilities of using atomic ground states to study spin relaxation using optical excitation has been demonstrated in the context of optical pumping [14] and more recently by the demonstration of spin nutation [15] and spin echoes involving ground-state Zeeman sublevels placed in a transverse field gradient [16].

Here, we describe a series of coherent transient experiments involving coherence grating echoes following proposals in recent work [3,4] in Doppler broadened Rb vapor at room temperature. A spatially modulated coherence is created between $\Delta m=2$ magnetic sublevels of the $F=3$ ground state in ^{85}Rb by an excitation pulse that consists of two opposite circularly polarized traveling waves with wave vectors \mathbf{k}_1 (with σ^- polarization) and \mathbf{k}_2 (with σ^+ polarization) at

an angle θ (\sim few mrad). Figure 1(a) shows a simplified level diagram of the atomic system. The pulses are tuned to the peak of the Doppler profile of the $F=3 \rightarrow F=4'$ transition. The coherence grating has a spatial periodicity $2\pi/\Delta k \sim 2\pi/k\theta$, where $\Delta k = |\mathbf{k}_1 - \mathbf{k}_2|$, $k = |\mathbf{k}_1| = |\mathbf{k}_2|$, and the excitation wavelength $\lambda = 2\pi/k$. The grating dephases due to thermal motion when the atoms move a distance of the order of the grating spacing, i.e., on a time scale $2\pi/ku\theta$ where u is the root-mean-square (rms) component of velocity transverse to the direction of excitation. We observe the grating by applying a σ^+ polarized “readout” pulse along \mathbf{k}_2 . This results in a coherent superposition of ground and excited states, which radiates with σ^- polarization along \mathbf{k}_1 (magnetic grating free induction decay or MGFID). A second excitation pulse applied at time $t=T$ after the first pulse causes the grating to rephase on the same time scale $2\pi/ku\theta$ and results in a magnetic grating echo (MGE) at $t=2T$. If the excitation pulses were counterpropagating, the MGE duration ($1/\Delta ku$) would be sensitive to the longitudinal velocity distribution, i.e., in this case, u would be the root-mean-square velocity component along the direction of the excitation.

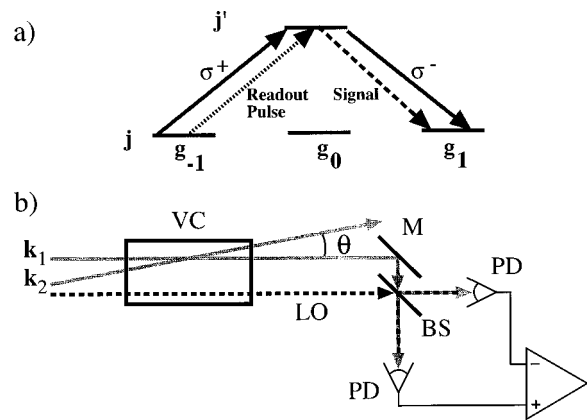


FIG. 1. (a) Simplified level diagram of atomic system. (b) Schematic of the experimental setup: VC is the vapor cell, LO the local oscillator, M the mirror, BS the beam splitter, PD the photodiode, \mathbf{k}_1 and \mathbf{k}_2 label the excitation beams and readout pulse (\mathbf{k}_2). $\theta \sim$ few mrad.

When the excitation pulses are resonant with the atomic transition, as is the case for the experiments described in this paper, MGFID and MGE signals can be generated from an initially equilibrium distribution of ground-state sublevels. Spontaneous and stimulated emission during the first excitation pulse produce the differences in population necessary to establish a coherence between sublevels. For excitation pulses sufficiently far from resonance (such that spontaneous emission can be neglected), it is first necessary to create a nonequilibrium distribution of magnetic sublevels [3], as can be done by optical pumping.

The experiments pertain to a Doppler broadened column of vapor of optical depth $\alpha_0 L < 1$ at room temperature. The temperature inferred from the duration of the echo (~ 200 ns for $\theta \sim 10$ mrad) demonstrates the accuracy of this method for determining the transverse velocity distribution. Results of a similar experiment have been used to determine sub-Doppler temperatures in trapped atoms [12]. The MGE lifetime, defined as the time T between excitation pulses at which the amplitude of the signal is half its maximum, was measured as a function of the beam radius. The lifetime was found to be the same as the transit time of the atoms through the laser beam. In the presence of Ar gas, the echo lifetime is shortened, allowing us to measure the collision cross section between Rb and Ar.

Figure 1(b) shows a schematic of the experimental setup. The opposite circularly polarized excitation pulses (50 to 100 ns in duration) are generated by two acousto-optic modulators (AOM's), which diffract light from a cw Ti: sapphire laser. A common rf oscillator operating at 220 MHz is used to drive both AOM's, and the time interval between pulses is controlled by delay generators. Pulses with wave vectors \mathbf{k}_1 and \mathbf{k}_2 are applied at a small angle (a few mrad) on resonance with the peak of the Doppler profile of the $F=3 \rightarrow F'=4$ transition. The MGFID and MGE signals are observed by applying a 500 ns readout pulse along \mathbf{k}_2 . The signal scattered along \mathbf{k}_1 is combined with the undiffracted cw light from the \mathbf{k}_1 AOM ("optical local oscillator") on a pair of high speed (~ 1 ns rise time) Si *p-i-n* photodiodes in a balanced detector arrangement. The optical local oscillator is 220 MHz above resonance (tuned to the wing of the Doppler profile), and spatially separated from the \mathbf{k}_1 beam by ~ 1 cm in the Rb cell. The 220-MHz signal from the detector is mixed with a reference signal from the rf oscillator in a quadrature demodulator. The low-frequency outputs of the demodulator, which represent the real and imaginary amplitudes of the scattered electric field, are recorded on a digitizing oscilloscope. The Rb vapor is contained in a homemade cell with 5-cm-diameter pyrex windows that is connected to a Rb reservoir and a pumping station. The walls of the cell are at ambient room temperature. We have used cells of length 5 cm or 10 cm and the optical depth $\alpha_0 L$ was varied between 0.1 and 1. The cell is shielded by several layers of Mumetal foil, reducing the residual magnetic fields to < 10 mG.

Because of the Doppler shift, only those atoms with a small velocity component along the excitation direction ($\mathbf{k}_{1,2} \cdot \mathbf{v} < 1/t_{\text{pulse}}$, for atomic velocity \mathbf{v} and pulse duration t_{pulse}) are resonant with the laser fields and contribute to the signal. All of these atoms satisfy the "two-photon resonance condition" for the transition between ground-state magnetic

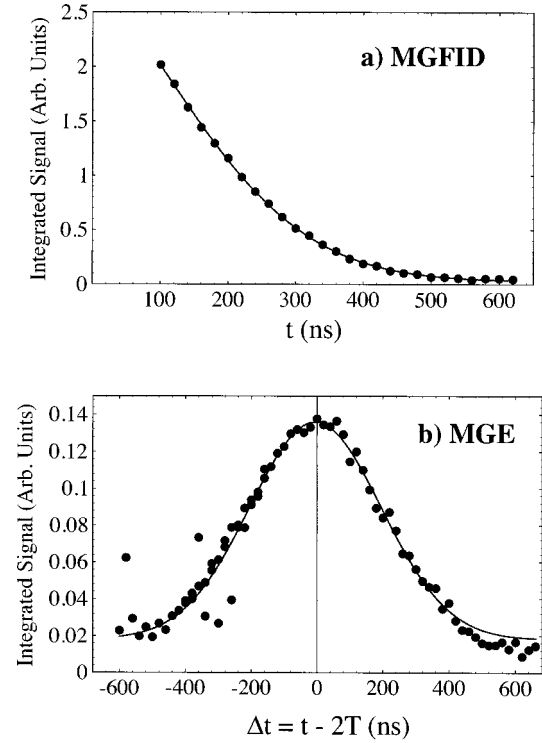


FIG. 2. MGFID and MGE obtained by varying "readout" pulse delay; $\theta = 3.6$ mrad; $\alpha_0 L \sim 0.7$. Decay time from Gaussian fits: 292 ns in (a), and 284 ns in (b). $T = 1 \mu\text{s}$ in (b).

sublevels. This follows from the fact that the frequency width of this resonance is $k\theta u/2\pi \sim 3$ MHz ($\theta = 10$ mrad, $u = 240$ m/s), which is smaller than the bandwidth of the pulses ($1/t_{\text{pulse}} \sim 10$ MHz). Predictions for the duration of the MGFID and MGE were obtained in [3] under the condition $\tau \gg \min[1/\Delta, \tau_N]$ where Δ is the detuning from the excited state and $\tau_N \approx 27$ ns is the excited-state lifetime. For small angle excitation, these results predict that the size of the MGFID and MGE as a function of time t will be a Gaussian of half width at half maximum (HWHM) $\tau_w = 2/ku\theta$.

Figure 2 shows the MGFID and the MGE at a fixed separation T between excitation pulses. The pulses have Gaussian spatial profiles. Their peak intensities correspond to Rabi frequencies $\Omega \sim 5\Gamma$ where Γ is the radiative rate of the $F'=4$ excited state ($3.7 \times 10^7 \text{ s}^{-1}$). Each data point is obtained by applying an intense readout pulse ($\Omega \sim 5\Gamma$) whose time delay can be varied with respect to the excitation pulses. The complex amplitudes of the signal obtained by averaging 300 repetitions of the experiment are squared, and integrated. Each data point is the square root of this quantity, which is proportional to the magnitude of the electric field. Alternatively, the entire envelope of these signals can be observed by applying a weak, suitably long, readout pulse ($\Omega \sim \Gamma$).

Representative Gaussian fits to the MGFID and MGE are shown in Figs. 2(a) and 2(b). The fits are of the form $\exp[-(ku\theta/2)^2 t^2]$ and allow us to infer the rms transverse velocity u . The inferred temperature is in agreement with the temperature of the cell walls measured with a thermocouple (298 K) and typically within 5% of the value determined by the thermocouple. This error is consistent with our uncertainty in the determination of θ . We have also verified that

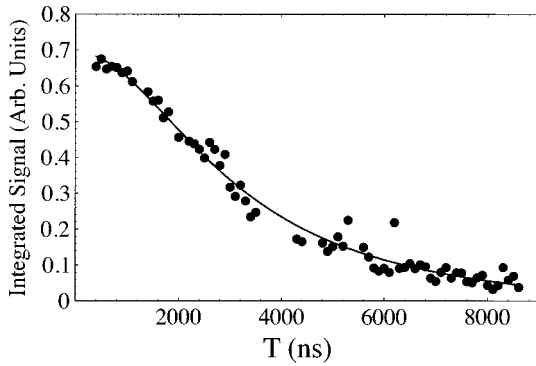


FIG. 3. MGE lifetime showing Lorentzian fit for a beam radius $R_x=0.7$ mm.

duration of the MGFID and MGE signals scales as $1/\theta$ as expected. When the density n_{Rb} was varied, the echo intensity was found to scale quadratically, which is a signature of coherent scattering. Larmor oscillations were observed in the MGE when a magnetic field was applied along the direction of excitation. The frequency of these oscillations was found to correspond to a splitting between magnetic sublevels separated by $\Delta m=2$, demonstrating that the observed signal involves a $\Delta m=2$ coherence between these sublevels. Since the excitation pulses have the same frequency in these experiments, the oscillation in the echo amplitude occurs at the frequency difference between magnetic sublevels induced by the field. We have also observed echoes involving $\Delta m=1$ coherences using excitation pulses with orthogonal linear polarizations.

In general, the amplitude of the MGE signal will depend on the pulse separation T . We refer to this dependence as the *echo envelope*. The echo envelope depends on the atom field coupling defined by the spatial profiles of the excitation and readout pulses as well as the velocity distribution. For a Maxwell-Boltzmann velocity distribution and Gaussian laser beams with radius R (at $1/e$ of maximum intensity), the echo envelope is predicted to be a Lorentzian whose HWHM is proportional to R/u with proportionality constant close to unity. The exact value of the proportionality constant is predicted to depend on the pulse intensity [17]. The Lorentzian dependence of the envelope of the echo *amplitude* (proportional to the electric field) is consistent with the results of [18], where the envelope of the echo *intensity* (proportional to the light intensity) was found to be the square of a Lorentzian.

The MGE lifetime (defined as the time T between excitation pulses at which the amplitude of the signal is half its maximum) was determined by increasing the separation T and measuring the echo amplitude at $t=2T$. These measurements were recorded with $\alpha_0 L \sim 0.06$ to ensure that collisions between Rb atoms were negligible over the time scale of the experiment. A Lorentzian fit to the data is shown in Fig. 3 for a beam size $R=0.7$ mm. The spatial profiles of the beams along \mathbf{k}_1 and \mathbf{k}_2 were determined from Gaussian fits to intensity profiles obtained by scanning a $100 \mu\text{m}$ pinhole along the vertical and horizontal directions. The MGE lifetime is plotted as a function of the smaller of the (horizontal) beam radii R_x in Fig. 4. The error bars ($\pm 20\%$) were estimated from the statistical variation in the data for a given beam size. The best fitting straight line to the data shows that

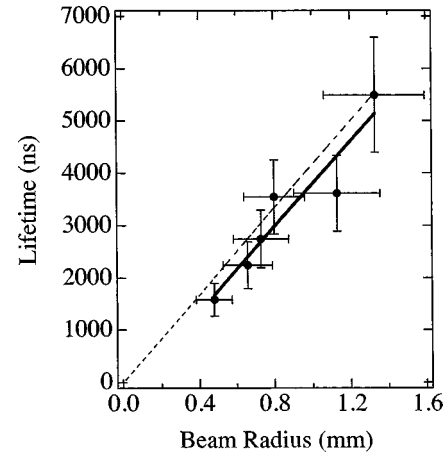


FIG. 4. MGE lifetime as a function of beam radius; best fit to data (solid line) has slope $4.1 \mu\text{s}/\text{mm}$ and offset $-0.3 \mu\text{s}$; R/u for $u=240$ m/s has a slope of $4.1 \mu\text{s}/\text{mm}$ (dashed line).

the MGE lifetime is in agreement with the transit time of atoms through the laser beam which is estimated as $\tau_R = R/u$ (dashed line). However, a detailed comparison with predictions [17] that relate the dependence of the lifetime on the excitation intensity are not possible on account of the experimental uncertainty.

The spatial periodicity of the induced coherence makes it possible to obtain information about velocity changing collisions in the presence of a buffer gas. These collisions will reduce the MGE lifetime. We measured the effect of Ar gas (at a pressure of a few milliTorr) on the MGE lifetime in the following manner. The echo envelope without Ar was first measured for a fixed beam size and optical depth (~ 0.7), and the data were fit by a Lorentzian $L_0(T)$ (see, for example, Fig. 3). The experiment was then repeated at various Ar pressures. In each case, the parameter Γ_c was determined by fitting the function $L_0(T)\exp(-\Gamma_c T)$ to data while holding other parameters fixed. This allowed us to measure the collisional rate Γ_c for collisions between Rb and Ar atoms in their respective ground states. Figure 5 shows a plot of Γ_c as a function of Ar pressure, which was fit to a straight line. The cross section was inferred from the slope of the best fitting straight line, $\Gamma_c(n_{\text{Ar}}) = 2\sigma v_{\text{rel}} n_{\text{Ar}}$. Here, n_{Ar} is the Ar density ($n_{\text{Ar}} \gg n_{\text{Rb}}$), σ is the collision cross section, and v_{rel} is the relative velocity between Rb and Ar determined from the temperature. The measured cross section ($1.2 \times 10^{-14} \text{cm}^2 \pm 20\%$) was found to be the same for $^{85}\text{Rb}(F=3)$ and

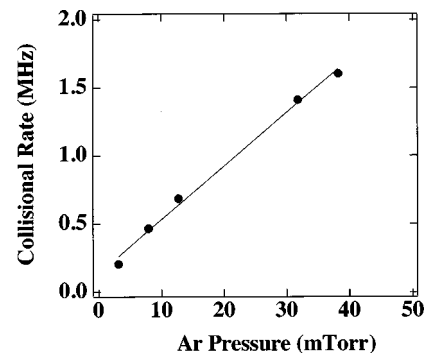


FIG. 5. Collisional rate Γ_c vs Ar pressure.

$^{87}\text{Rb}(F=2)$ ground states. We note that the collisional cross section for a change in the Rb hyperfine ground state is orders of magnitude smaller [14]. In addition, there is no collisional redistribution among the magnetic sublevels of the $F=3$ ground state [14]. Thus, σ is associated with velocity changing collisions. Only atoms that have undergone a collisional velocity change $\delta v < v'$ contribute to the echo. Here, $v' = (1/T)(2\pi/k\theta)$ is the velocity defined by the grating spacing ($v' \sim 25$ m/s for $\theta = 10$ mrad, $T = 3$ μs). The collisional velocity change due to diffractive scattering [19] $\delta v_{\text{diff}} = 2(2\pi)^{0.5}\hbar/M_{\text{Rb}}\sigma^{0.5} \sim 3.5$ m/s for the measured cross section and is much smaller than v' . Thus, the collision may be modeled by classical scattering at small impact parameters [19,20]. As a result, this experiment is not sensitive to small angle diffractive scattering associated with large impact parameters. For classical scattering, Ref. [20] predicts that σ should scale as $T^{1/3}$. The data, however, suggest that σ is independent of T . The behavior of σ at smaller values of T that may reveal a $T^{1/3}$ dependence is an issue for further investigation. It would be possible to achieve sensitivity to smaller velocity changes with counterpropagating excitation pulses. We note that the measured collisional rate is comparable to the collisional rate reported in [21]. Detailed studies of our measurements will be presented elsewhere. Previous echo experiments that have demonstrated sensitivity to small velocity changes for magnetic order in vapors are described in Ref. [22].

In conclusion, we have presented experimental observations of coherence grating echoes involving superpositions of magnetic sublevels of a single hyperfine ground state. Measuring the duration of the echo is an accurate and simple method of inferring the velocity distribution. In the absence of collisions, the echo lifetime has been shown to be limited only by the transit time of the atoms across the interaction region. The shortening of the lifetime in the presence of Ar gas has been utilized for measuring the elastic Rb-Ar collision

cross section. It would be useful to improve the sensitivity to smaller velocity changes using counterpropagating pulses. The effect of optically pumping the sample before the experimental pulse sequence may result in an improvement in signal to noise and also remains to be studied. We have recently observed the destruction of MGFID at low buffer gas concentration. At high perturber concentrations, the motion of Rb atoms is described by diffusion and a collisional revival of the signal occurs. Details of this experiment will be presented separately.

In related experiments in trapped atoms we have observed the MGFID and MGE with the excitation pulses applied at a small angle (“forward”) as well as close to 180° (“backward”) [12]. Temperatures inferred were well below the “Doppler” limit and show the applicability of this technique for measuring velocity distributions of cold atoms [23,24]. The amplitude of the backward echo measured as a function of the time delay T between excitation pulses was observed to be modulated at the atomic recoil period [12] (the time taken by the atoms to move one grating period due to the velocity acquired by the absorption and stimulated emission of a photon from one beam into the other). This effect was recently demonstrated in an atomic beam [25] and may be used for a precision measurement of h/m and g . Measurements of velocity distributions of cold atoms, and precision measurements of h/m and g have already been reported in [10] using an interferometer that uses pulsed standing waves. Other applications, which include magnetic imaging of the trapped sample and sensitivity to magnetic fields, will be presented elsewhere.

We are grateful for helpful discussions with Jayson Cohen, Boris Dubetsky, and Paul Berman of the University of Michigan. We acknowledge the financial support of NYU, the U.S. Army Research Office through Grant No. DAAG55-97-0113, and the Packard Foundation.

-
- [1] B. Dubetsky, P. R. Berman, and T. Sleator, *Phys. Rev. A* **46**, R2213 (1992).
 [2] R. Friedberg and S. R. Hartmann, *Phys. Rev. A* **48**, 1446 (1993).
 [3] B. Dubetsky and P. R. Berman, *Laser Phys.* **4**, 1017 (1994).
 [4] B. Dubetsky and P. R. Berman, *Appl. Phys. B: Lasers Opt.* **59**, 147 (1994).
 [5] J. Schmidt, P. R. Berman, and R. G. Brewer, *Phys. Rev. Lett.* **31**, 1103 (1973).
 [6] T. Mossberg, A. Flusberg, R. Kachru, and S. R. Hartmann, *Phys. Rev. Lett.* **42**, 1665 (1979).
 [7] R. A. Forber, Li. Spinelli, J. E. Thomas, and M. S. Feld, *Phys. Rev. Lett.* **50**, 331 (1983).
 [8] I. D. Abella, N. A. Kurnit, and S. R. Hartmann, *Phys. Rev.* **141**, 391 (1965).
 [9] T. W. Mossberg, R. Kachru, E. Whittaker, and S. R. Hartmann, *Phys. Rev. Lett.* **43**, 851 (1979).
 [10] S. B. Cahn, A. Kumarakrishnan, U. Shim, T. Sleator, P. R. Berman, and B. Dubetsky, *Phys. Rev. Lett.* **79**, 784 (1997).
 [11] R. Kachru, T. W. Mossberg, E. Whittaker, and S. R. Hartmann, *Opt. Commun.* **31**, 223 (1979).
 [12] A. Kumarakrishnan, S. B. Cahn, U. Shim, and T. Sleator, *Phys. Rev. A* **58**, 3387 (1998).
 [13] M. Weitz, T. Heupel, and T. W. Hansch, *Phys. Rev. Lett.* **77**, 2356 (1996).
 [14] W. Happer, *Rev. Mod. Phys.* **44**, 169 (1972).
 [15] D. Suter, M. Rosatzin, and J. Mlynek, *Phys. Rev. A* **41**, 1634 (1990).
 [16] M. Rosatzin, D. Suter, and J. Mlynek, *Phys. Rev. A* **42**, 1839 (1990).
 [17] J. L. Cohen and P. R. Berman, *Phys. Rev. A* **54**, 5262 (1996).
 [18] J. E. Thomas and R. A. Forber, *Opt. Lett.* **9**, 56 (1984).
 [19] P. R. Berman, T. W. Mossberg, and S. R. Hartmann, *Phys. Rev. A* **25**, 2550 (1982).
 [20] J.-C. Keller and J.-L. Le Gouet, *Phys. Rev. Lett.* **52**, 2034 (1983).
 [21] K. E. Gibble and A. Gallagher, *Phys. Rev. A* **43**, 1366 (1991).
 [22] A. Yodh, T. W. Mossberg, and J. E. Thomas, *Phys. Rev. A* **34**, 5150 (1986); J. E. Thomas, A. P. Ghosh, and M. A. Attili, *ibid.*

- 33**, 3029 (1986); A. P. Ghosh, C. D. Nabors, M. A. Attili, and J. E. Thomas, Phys. Rev. Lett. **54**, 1794 (1995).
- [23] D. R. Meacher, D. Boiron, H. Metcalf, C. Salomon, and G. Grynberg, Phys. Rev. A **50**, R1992 (1994).
- [24] M. Kozuma, Y. Imai, K. Nakagawa, and M. Ohtsu, Phys. Rev. A **52**, R3421 (1995).
- [25] M. Weitz, T. Heupel, and T. W. Hansch, Europhys. Lett. **37**, 517 (1997).